Narrowband and wideband EMW path loss in underwater wireless sensor network

Hanisah Mohd Zali
School of Electrical Engineering, College of Engineering, Universiti Teknologi MARA, Melaka, Malaysia
Mohd Khairil Adzhar Mahmood and Idnin Pasya
Microwave Research Institute, Universiti Teknologi MARA, Shah Alam, Selangor, Malaysia
Miyuki Hirose
School of Science and Technology for Future Life, Tokyo Denki University – Tokyo Senju Campus, Adachi-ku, Japan, and
Nurulazlina Ramli
Faculty of Engineering, Built Environment and Information Technology, SEGi University College Kota Damansara, Petaling Jaya, Malaysia

Abstract

Purpose – Utilization of electromagnetic wave (EMW) sensors in an underwater environment has the potential to increase the data rate compared to acoustic-based sensors because of the ability to use larger signal bandwidth. Nevertheless, EMW signals has the drawback of large signal attenuation in underwater, attributed to the high relative permittivity and conductivity of water compared to the atmosphere, hence employment of wide signal bandwidth is necessary to balance the data rate-attenuation trade-off. The purpose of this paper is to analyze the characteristics of both narrowband and wideband EMW signal propagation underwater and devise a path loss model for both cases.

Design/methodology/approach – Path loss measurement was conducted using a point-to-point configuration in a laboratory water tank while transmitting narrowband and wideband signals between a pair of wideband underwater antennas. The wideband underwater antennas use buffer-layer structures as the impedance matching layer to optimize the antenna performance when operating underwater. The path loss for narrowband signal was modeled using a multi-layer propagation equation in lossy medium considering losses at the medium boundaries. For the case of the wideband signal, a modified version of the model introducing power integration over bandwidth is adopted. These models were formulated through numerical simulations and verified by measurements.

Findings – The measured narrowband path loss marked an 80 dB attenuation using 800 MHz at 2 m distance. The proposed narrowband model agrees well with the measurements, with approximately 3 dB modeling error. Utilization of the proposed wideband path loss model resulted in a reduction of the gradient of the path loss curve compared to the case of the narrowband signal. The measured wideband path loss at 2 m distance underwater was approximately −65 dB, which has been shown to enable a working signal-to-noise ratio of 15 dB. This proves the potential of realizing high data rate transmission using the wideband signal.

Originality/value – The paper proposed a wideband propagation model for an underwater EMW sensor network, using power integration over bandwidth. The effectiveness of using wideband EMW signals in reducing path loss is highlighted, which is seldom discussed in the literature. This result will be of useful reference for using wideband signals in designing a high data rate transmission system in underwater wireless sensor networks, for example, in link budget, performance estimation and parameter design of suitable transmission scheme.

Keywords Sensor networks, Wideband, Narrowband, Path loss, Underwater antenna, Underwater sensors, Underwater communication

Paper type Research paper

Introduction

Recent advancement of internet-of-things technology has led to the development of various underwater systems comprise of multiple intelligent sensors for environmental monitoring, exploration of natural resources and also modern aquaculture activities. As shown in Figure 1, some parts of the underwater network still rely on "wired" connections between the sensors, network controller and the operators or the central processing unit, limiting the operating range and location of sensors, while prone to cable breakdowns. Therefore, there is a need to use wireless sensor networks in these underwater applications.

Underwater communications, telemetry and positioning applications commonly use acoustic-based sensors and systems

The current issue and full text archive of this journal is available on Emerald Insight at: **https://www.emerald.com/insight/0260-2288.htm**

Sensor Review
42/1 (2022) 125–132
© Emerald Publishing Limited
[ISSN 0260-2288]
[DOI 10.1108/SR-04-2021-0128]

The author would like to thank the Exploratory Research Grant Scheme under the Ministry of Higher Education of Malaysia, Grant number FRGS/1/2015/TK04/UITM/02/32 for partly funding this project.
Received
Ministry of Higher Education of Malaysia.

Received 21 April 2021
Revised 14 September 2021
Accepted 15 October 2021

Figure 1 Underwater IoT network using underwater sensors

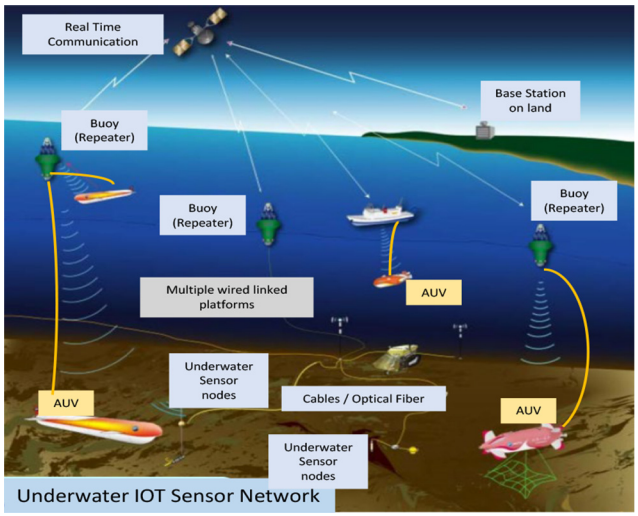

(Van Walree and Otnes, 2013). As an acoustic signal is susceptible to propagation characteristics from background medium and has limited bandwidth, radio signal using electromagnetic wave (EMW) is being investigated as the alternative data transmission mechanism among underwater sensors to provide a higher data rate. Radio signal traveling in free space suffer attenuation due to the spreading of its energy as the signal moves through space and this becomes more severe in the underwater environment due to losses brought by the high permittivity and conductivity of the propagation media (Che *et al.*, 2010). Motivated by the potential benefits of EMW systems, re-evaluation of underwater communication using EMWs has been recently conducted by many researchers in various institutions. For example, in Al-Shamma'a (2004), an experimental measurement in sea-water at several narrowband frequencies up to 65 MHz in a line-of-sight (LOS) configuration was carried out in Liverpool University laboratory, reported an 80 dB path loss at 1 m distance.

Yoshida *et al.* (2015) published their investigation on signal attenuation using a 10 MHz small loop narrowband antenna, recording a 90 dB attenuation at 2 m, however, their result had some disagreement with theoretical calculations.

Another study at higher frequencies reported some feasibility of using EMW in underwater systems using the unlicensed the industrial, scientific, and medical (ISM) frequency bands, which are 6.7 MHz, 433 MHz and 2.4 GHz (Abdou *et al.*, 2011). Investigations on alternative underwater EMW propagation other than LOS are also reported, such as in Nie *et al.* (2018), where a sea-rock-layer propagation model is analyzed by simulation, using narrowband signal up to 150 kHz. The proposed model marked a 1/20 path loss compared to the LOS configuration. These achievements indicated potential usage of EMW signals to increase the transmission data rate, especially in short-range communications. In addition, Takizawa *et al.* managed to obtain a 1 Mbps bit rate at 1 MHz, using a 2×2 MIMO configuration for 1 m distance in seawater (Takizawa *et al.*, 2021).

Another regime of underwater EMW study explores the development of underwater antennas (M. Zali *et al.*, 2018; Aboderin *et al.*, 2017), and underwater-optimized wireless transmission schemes, such as usage of MIMO communications and orthogonal frequency division multiplexing (OFDM) transmission scheme (Trung and Van Duc, 2011), indicating more research interest to realize high data rate EMW communication in the underwater environment.

The above-mentioned research mostly focused on the propagation of narrowband EMW signals, development of antennas operating at narrowband frequencies and narrowband transmission schemes. It is a fact that the utilization of EMW signals underwater produces large signal attenuation. This will cause any wireless system to operate at a low signal-to-noise ratio (SNR), resulting in higher transmission errors and a reduced transmission rate. Here, the utilization of wider signal bandwidth enables increased channel capacity (Shannon limit theorem) and ultimately provides the potential to increase the overall data rate of the system. Selection of appropriate parameters in designing a wideband wireless transmission system may provide better performance in short-range underwater communications. Nevertheless, resources, data and investigation on wideband signal propagation in the underwater environment are rarely discussed, limiting the development in this area.

Drove by this motivation, this paper presents an investigation on the path loss of both narrowband and wideband signals in an underwater environment, to study the difference in the propagation characteristics between them and later on highlight the frequency diversity effect brought by utilization of wider signal bandwidth on the path loss curve. The main contribution of this paper is to model the underwater path loss for both narrowband and wideband electromagnetic (EMW) through simulation and measurement, and show the effectiveness of using a wideband signal in reducing the path loss curve gradient.

The remainder of this paper is organized as follows. Section 2 explains the underwater antennas used in the study, the measurement setup and the derivation of path loss models for both narrowband and wideband cases. Section 3 discusses the simulation and measurement results, starting with the analysis of narrowband path loss and its comparison ith a theoretical calculation based on the Maxwell equation for propagation in a multi-layer lossy medium. Next, the path loss for the wideband signal is analyzed and compared with its narrowband counterpart. Section 4 presents a comparison of path loss with related works in literature and the potential impact of using wideband signal on underwater transmission link budget. Finally, concluding remarks are presented in Section 5.

Measurements setup and path loss model

Wideband underwater antenna

This study uses a pair of wideband microstrip patch antennas using buffer-layer structures developed in previous works for path loss measurement (M. Zali *et al.*, 2018). The antenna is submerged in a container filled with a liquid-based material (M. Zali *et al.*, 2019), as depicted in Figure 2. The buffer layer acts as a matching layer to optimize the antenna impedance matching in an underwater environment throughout the wide bandwidth. As reported in previous work (M. Zali *et al.*, 2019), using a buffer layer with relative permittivity between freshwater and air resulted in optimum radiation characteristics of the antenna. Simulation and measurement reported in the previous work indicated that relative permittivity of 8.5 is the

Figure 2 Illustration of the antenna design

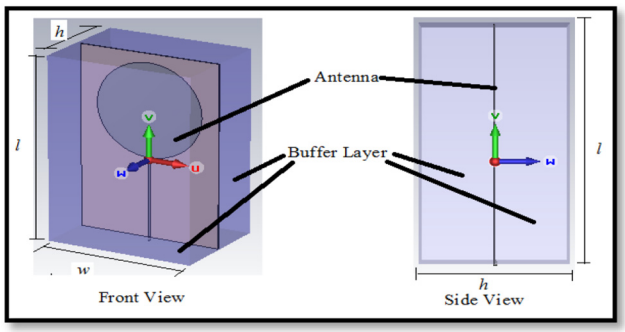

optimum value for the buffer layer. This study used a mixture of methyl-acetate and distilled water by a ratio of 6:1 to obtain a buffer solution with relative permittivity of 8.5. The dimension of the antenna parameter is presented in Table 1. The size of the underwater buffer structure is designed to have a horizontal length approximating the size of the reactive near field region of the antenna. Based on simulations reported in previous work (M. Zali *et al.*, 2019), it was found that by using such size resulted in optimum radiation performance of the antenna. The utilization of the buffer layer introduces slightly higher attenuation compared to direct antenna contact with water, however, the higher antenna gain in buffer compensates for the additional loss. On the other hand, the wave velocity of the EMW signal in the buffer is higher compared to propagation in water (Refer to Appendix for a detailed explanation). The antenna has return loss around or below −10 dB from 200 to 1 GHz when operating in freshwater. Table 1 shows the overall size of the underwater antenna structure.

Figure 3 shows the return loss, S_{11} performance of the underwater antenna, measured while submerging the antenna underwater. It can be observed that the return loss is below −10 dB over a wide bandwidth from 200 MHz to 800 MHz, making it suitable for broadband, wideband and ultra-wideband systems. The antenna gain when operating in underwater was 0 to −6 dB over the wide bandwidth.

Path loss measurement setup and procedure

The path loss characteristic of the narrowband and wideband propagation were analyzed based on experimental measurements in a laboratory water tank, by taking the transmission loss S_{21} while varying the distance between the antennas. Figure 4 shows the measurement setup for the antenna underwater environment. The measurement is done inside the fibre-reinforced plastic water tank with dimensions $2.5 \times 1.5 \times 1$ m, filled with tap water. The antennas was aligned in a straight horizontal line facing each other. The antennas were submerged in the water, where their electrical centers were positioned at 0.8 m of height. The transmitting and receiving antennas are connected to Ports 1 and 2 of a vector network analyzer (VNA), respectively. The path loss is obtained by measuring the receiving signal power at Port 2 of the VNA while varying the distance between transmitting and receiving antenna. In this experiment, the distance was varied with 0.5 m step size up to 2 m of distance. Measurements were conducted in a wide frequency range, from 200 MHz to 800 MHz in 1 MHz of the interval using the frequency sweep function of the VNA. The measurement parameters are summarized in Table 2. It is worth to note that the path loss measurement was carried out at a frequency range below 1 GHz, taking into account the possibility of using existing industrial wireless standards at lower ISM bands, i.e. at 433 MHz (Abdou *et al.*, 2011), rather than using systems at higher frequencies which will generate higher signal attenuation underwater. The measurement environment is also simulated using the same parameters in CST Microwave Studio, where the S_{21} is observed and compared with the measurement results. The simulation uses the parameters listed in Table 2.

Table 1 Dimension of the designed wideband underwater antenna

Antenna Parameter	Dimension Parameter	Dimension (mm)
Dimension	Width, *w*	200
	Length, *l*	290
	Thickness. *H*	200

Underwater path loss model

Figure 5 shows the setup for underwater path loss measurement. The path loss for the environment under study is considered a plane wave traveling inside a homogeneous lossy medium (water), from the transmitting antenna to the receiving antenna.

Figure 3 Comparison of simulated and measured S11 of the wideband underwater antenna

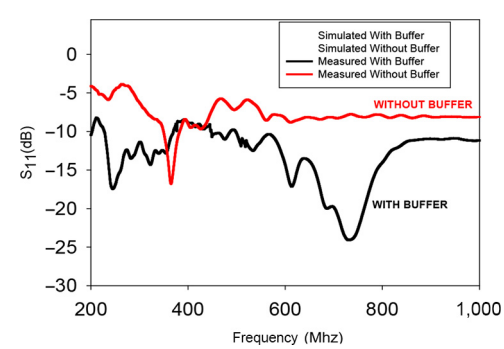

Figure 4 Illustration of S21 setup for simulated and experimental study

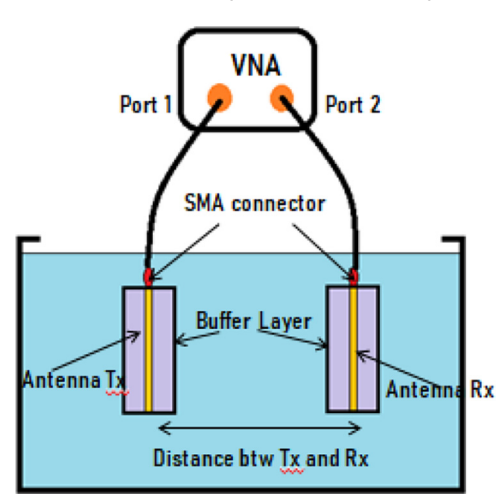

Table 2 Parameters used in simulation

Simulated materials Parameters	Symbol	Value
Buffer Structure	Permittivity, εr_b	8.85
	Permeability, μ_b	1
	Conductivity, σ_b	0.007 S/m
Water Background	Permittivity, εr	78.4
	Permeability, μ	1
	Conductivity, σ	0.0005 S/m

In addition, as the antenna is using a buffer-layer structure, the wave also propagates from the buffer-layer into the water at the transmitting side and vice-versa at the receiving side. Hence, it is treated as a multi-layer propagation consisting of three separate regions (Figure 6).

The path loss for any selected narrowband frequency, therefore, takes into account the propagation losses in both water and buffer-layers, and the transmission losses occurring at the boundary of the mediums. The total path loss is defined as follows:

$$PL = \alpha_p + \alpha_b + L + G_T + G_R \tag{1}$$

where α_p and α_b are the propagation losses in water and buffer-layer, respectively, L is the transmission losses at boundaries and G_T and G_R are the transmitting and receiving antenna gain, respectively. Here, α_p and α_b is given by:

$$\alpha_p = 10\log_{10}\left(e^{-2\alpha_1 d_1}\right) \tag{2}$$

$$\alpha_b = 10\log_{10}\left(e^{-2\alpha_2 d_2}\right) \tag{3}$$

where d_1 and d_2 correspond to the propagation distance in water and the buffer-layer, respectively. Furthermore, α_1 and α_2 are the attenuations constant in both of the respective mediums:

$$\alpha_1 = \omega\sqrt{\frac{\mu\varepsilon}{2}\left(\sqrt{1+\left(\frac{\sigma}{\omega\varepsilon}\right)^2} - 1\right)} \tag{4}$$

and

Figure 5 Measurement of path loss antenna in underwater condition

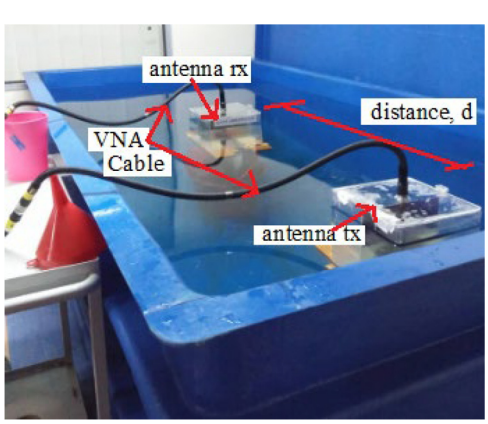

Figure 6 Multi-layer propagation model for the underwater path loss

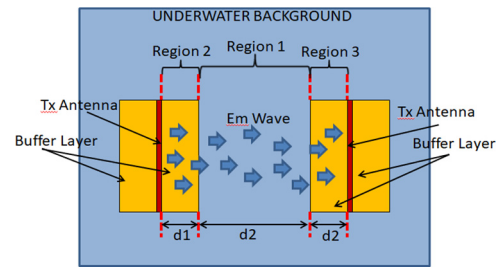

$$\alpha_2 = \omega\sqrt{\frac{\mu_2\varepsilon_2}{2}\left(\sqrt{1+\left(\frac{\sigma_2}{\omega\varepsilon_2}\right)^2} - 1\right)} \tag{5}$$

Here, ε and ε_2 are the relative permittivity, σ and σ_2 are the conductivity and μ and μ_1 are the relative permeability of water and buffer-layer, respectively. The transmission losses at the boundaries L is defined as follows:

$$L = 10\log_{10}\left(T^2 * \mathrm{Re}\left(\frac{\eta_1}{\eta_2}\right)\right) \tag{6}$$

where the transmission coefficient T is given by [13]

$$T = \frac{E_t}{E_i} = \frac{2\eta_2}{\eta_1 + \eta_2} \tag{7}$$

where η is the intrinsic impedance given by:

$$\eta = \sqrt{\frac{\mu}{\varepsilon}} \tag{8}$$

and the E_t is the transmitted electric field and E_i is the incident electric field.

The path loss for wideband signal occupying selected bandwidth can be modeled by imposing a power integration over the selected bandwidth in equation (1). The wideband path loss PL_w is, therefore, represented by the below equation:

$$PL_w = \frac{1}{f_H - f_L}\int_{f_L}^{f_H} PL_{\Delta f}\, d\Delta f \tag{9}$$

where $PL_{\Delta f}$ is the path loss at the fth frequency interval, f_H and f_L are the highest and lowest frequencies, respectively. Upon calculating $PL_{\Delta f}$ at a selected narrowband frequency, $\omega = 2\pi\Delta f$ is used, where Δf corresponds to the narrowband center frequency. For the sake of simplicity, other parameters such as relative permittivity, relative permeability and conductivity for both water and buffer-layer are considered as a flat value across the selected bandwidth.

Simulation and measurement result

This section discusses the results of measurement and simulated path loss for the environment under study. Path loss is initially analyzed against frequency for each narrowband frequency, and later on compared with the multi-layer

propagation model. Next, the wideband path loss will be discussed in terms of the path loss curve against propagation distance, with varying bandwidth.

Narrowband path loss against frequency

Figures 7 and 8 illustrate the measured path loss results against frequency, where measurements were taken from 200 to 800 MHz, at the interval of 1 MHz. The figures show how much do the signal attenuates with increasing frequency. From Figure 7, using a 200 MHz narrowband frequency for 0.5 m propagation distance gives approximately 25 dB of path loss. Using signals around 800 MHz signals at the same distance marked 50–55 dB path loss. Upscaling from 200 to 800 MHz marked approximately 25–30 dB increase in path loss. Similar trend is observed at 2 m propagation distance. The measurement result agrees with the simulated results.

Next, the measurement results if fitted over the proposed multi-layer propagation model. The comparison between the two is depicted in Figure 9. It was found that the measurements are at considerable agreement with the model, where minimal modeling error was observed.

The modeling error ΔPL, taken as

Figure 7 Comparison of simulated and measured S21 against frequency at distance 0.5 and 1.5 m

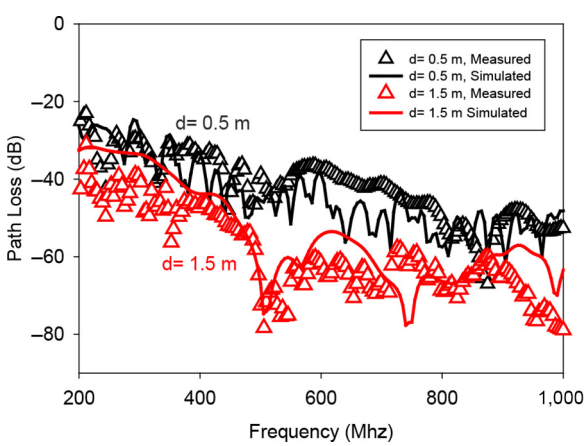

Figure 8 Comparison of simulated and measured S21 against frequency at distance 1.0 and 2.0 m

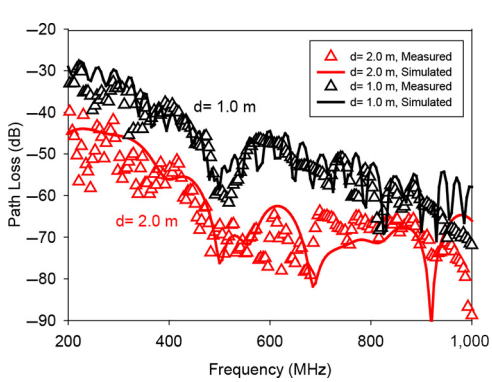

$$\Delta PL = |PL_{measured} - PL_{model}| \tag{10}$$

is shown in Figures 10 and 11. As shown in the figures, average modeling errors are around 5 dB for all narrowband frequencies, except when using narrowband frequencies from 500 to 650 MHz at 2 m distance (Figure 11). This is attributable to additional losses brought by multipath fading at the selected frequencies at that propagation distance, which could not be modeled by only looking at the receiving signal power. Assuming that multipath exists in the measurement setup, the receiving signal can be considered as a combination of the direct wave and several reflected waves from the water tank base and wall. The reflected waves may produce a destructive combination at a specific phase delay, which could introduce additional loss. When the distance is at 2 m, the receiving power of the direct wave is smaller compared to other distances, and hence, the effects of the additional losses became more significant. More detailed measurement and modeling using other parameters such as the delay profiles in the time domain, is necessary, which will be covered in subsequent publications.

Narrowband and wideband path loss against distance

This sub-section discusses the measured path loss against distance for both narrowband and wideband signals. Figure 12 presented the path loss at selected narrowband frequencies and

Figure 9 Comparison between measured and calculated path loss

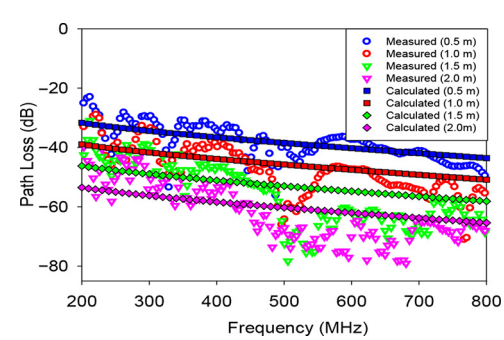

Figure 10 Modeling error for different narrowband frequency at 0.5 distance between Tx and Rx

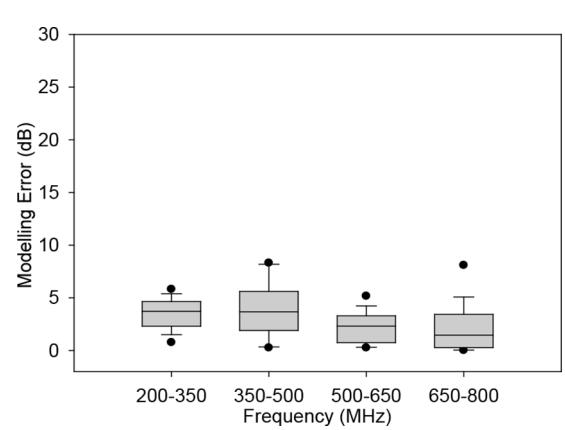

Figure 11 Modeling error for different narrowband frequency at 2.0 m distance between Tx and Rx

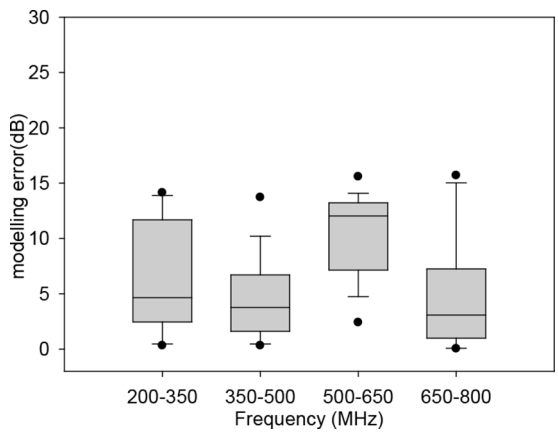

Figure 13 presented the wideband path loss curve for several different bandwidths (200 to 800 MHz). Both cases showed a similar trend of increasing path loss while increasing distance. According to Figure 12, underwater EMW transmission using narrowband frequencies from 200 to 300 MHz at 2 m distance produces path loss around 40–50 dB. This is in agreement with results from other works, such as in equation (3). On the other hand, path loss when using narrowband frequencies from 800 to 1 GHz at 2 m was approximately 80–90 dB. Comparing the path loss slope for all narrowband frequencies, it can be observed that the slope for at 200 MHz has a relatively lower gradient compared to, for example, a steeper slope at 600 MHz. A maximum path loss of 17 dB is observed at 600 MHz when changing the distance to 1 to 1.5 m, while the path loss is only around 5 dB at 200 MHz.

Figures 13 and 14 depict the path loss in the case of the wideband signal. It is shown that by taking the integration of receiving power over the selected bandwidth, the path loss slope was reduced. It can be seen from Figure 13 that when using larger bandwidth, for instance, 400 MHz and 800 MHz, the path loss increased 18 and 16 dB, respectively, when the distance was changed from 1 to 2 m. Using a narrowband signal at the same distance produced an approximately 30 dB increase in path loss. This reduction in path loss is attributed to the

Figure 12 Path loss against distance at selected narrowband frequencies

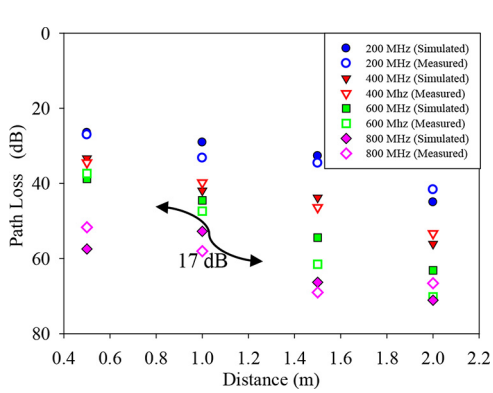

Figure 13 Comparison of measured path loss result while varying the bandwidth (center frequency fc = 600 MHz)

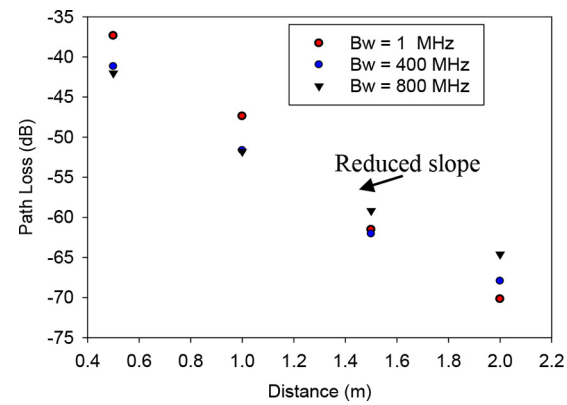

Figure 14 Comparison of simulated path loss result while varying the bandwidth (center frequency fc = 600 MHz)

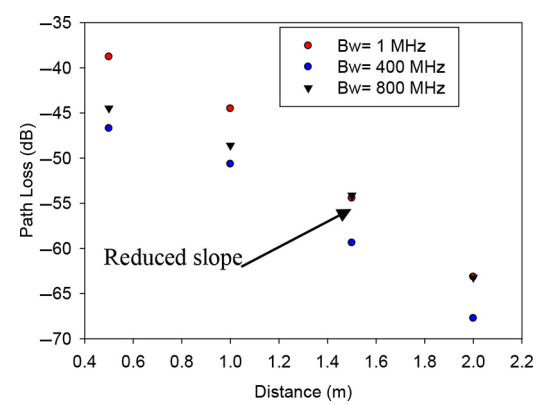

frequency diversity effect of the wideband signal. These results indicate an example of reduced signal attenuation when using wideband signals compared to narrowband in the underwater environment. While the frequency diversity effects is considered known characteristics in ultra-wideband propagation in terrestrial wireless communications, this report validated similar effects if a wideband signal is used in an underwater environment, putting forward its potential to realize a high data rate in short-range underwater communication systems.

Discussion

This section discusses the comparison between the proposed wideband path loss model with other works reported in the literature and the impact of the wideband path loss model on data rate improvements of underwater sensor networks. A comparison of measured path loss in fresh water-like mediums was carried out between the present work (this present paper) and narrowband path loss results from Hirose and Pasya (2020) and Abdou *et al.* (2011), in terms of path loss against distance (refer Table 3). From the table, it is shown that the measured path loss obtained when using wide signal bandwidth indicated reduced path loss, where approximately −65 dB compared to −110 dB and −90 dB from the other works.

Table 3 Comparison between the proposed wideband path loss and other narrowband path loss measurement results

Path loss measurements	Parameters	Path Loss	Path loss Slope
Present work	Propagation distance: 2 m Frequency: 200–800 MHz (Bandwidth 6.00 MHz)	−65 dB	9 dB/ m
Hirose and Pasya (2020)	Propagation distance: 4 m Frequency: 10 MHz	−110 dB	25 dB/m
Abdou *et al.* (2011)	Propagation distance: 1 m Frequency: 433 MHz	−90 dB	15 dB/m

Although the operating frequencies and propagation distance are different, the path loss obtained in the present work indicated a higher potential to realize a high performance EMW transmission scheme for underwater sensor networks. The present work marked a reduced path loss slope due to wideband frequency diversity, approximating 9 dB/m, compared to other works using narrowband signal, marking −25 dB/m and 15 dB/m.

Second, the impact on the link budget of an underwater transmission scheme is discussed. For example, a simple link budget for an underwater network is considered as below:

$$P_r = P_t + PL_{total} + G_T + G_R + (2 * G_{HPA}) \tag{11}$$

where P_r is the receiving power at the receiver, P_t is the transmitting power at the transmitting antenna, PL_{total} is the total path loss (underwater), G_T and G_R is the transmitting and receiving antenna gain and G_{HPA} is the gain of the high power amplifiers used at both the transmitter and receiver side. Assuming transmit power at 0 dB, the gains of the antennas are −5 dB and the G_{HPA} is 20 dBi and PL_{total} of −65 dB, P_r is estimated at −35 dB. If we consider a noise floor at the receiver at −50 dB, the working SNR is 15 dB. At this working SNR, a wideband transmission scheme such as an OFDM scheme using a quadrature phased shift keying modulation (Kaneko and Maehara, 2009) can operate at 10^{-5} bit-error-rate, which is sufficient for a transmission rate up to 10 Mbps. This shows the potential to realize high data rate communications.

Conclusion

This paper presented an evaluation of underwater EMW path loss for narrowband and wideband signals through actual measurements. The measurement was done in a laboratory water tank, using an underwater-optimized wideband antenna using a buffer layer structure. The narrowband path losses were modeled by a multi-layer propagation equation taking into account the propagation losses in both water and the buffer layers. The actual path loss measurement shows considerable agreement with the model for narrowband signals, with modeling errors around 3 dB for most cases. The authors recommend another model considering multi-path and delay profiles for more accurate analysis in future works. In addition, the wideband path loss was measured by using a power integration over bandwidth. Using wider signal bandwidth such as 400 MHz and 800 MHz (center frequency f_c = 600 MHz) marked a reduction in the gradient of the path loss curve, compared to the case of the narrowband signal. This result validated the frequency diversity effects of wideband propagation in the underwater environment. A link budget incorporating the measured wideband path loss was also shown to produce a working SNR of 15 dB, which is sufficient to realize a high transmission rate short-range wireless communication in the underwater environment.

References

Abdou, A.A., Shaw, A., Mason, A., Al-Shamma'a, A. and Cullen, J. W., S. (2011), "Electromagnetic (EM) wave propagation for the development of an underwater wireless sensor network (WSN)", *2011 Ieee Sensors*, pp. 1571-1574.

Aboderin, O., Pessoa, L.M. and Sagado, H.M. (2017), "Analysis of loop antenna with ground plane for underwater communications", *Oceans 2017 - Aberdeen*, Vol. 2017–Octob, pp. 1-6.

Al-Shamma'a, A., Shaw, A. and Saman, S. (2004), "Propagation of electromagnetic waves at MHz frequencies through seawater", *IEEE Transactions on Antennas and Propagation*, Vol. 52 No. 11, pp. 2843-2849.

Che, X., Wells, I., Dickers, G., Kear, P. and Gong, X. (2010), "Re-evaluation of RF electromagnetic communication in underwater sensor networks", *IEEE Communications Magazine*, Vol. 48 No. 12, pp. 143-151.

Hirose, M. and Pasya, I. (2020), "An HF channel measurement testbed for underwater/under-Seawater communications", *2020 International Workshop on Antenna Technology (iWAT)*, pp. 1-3.

Kaneko, R. and Maehara, F. (2009), "Theoretical derivation of bit error rate in MB-OFDM UWB system", *2009 Wireless Telecommunications Symposium, Prague, Czech Republic*, pp. 1-5.

M. Zali, H., Pasya, I., Ali, M.T. and Kobayashi, T. (2018), "Measurement of wideband microstrip underwater antenna performance with buffer layer structure", *2017 IEEE 13th Malaysia Int. Conference Communication. MICC 2017*, Vol. 2017–Novem No. Micc, pp. 48-52.

M. Zali, H., Pasya, I., Ali, M.T. and Mahmood, M.K.A. (2019), "Wideband microstrip antenna integrated with optimized buffer layer parameters for underwater wireless communication", *Journal of Electrical and Electronic System Research (JEESR)*, pp. 1-8.

Nie, Z.Q., Wang, S.L., Chen, D.H. and Deng, T. (2018), "Seabed-Rock-Layer electromagnetic communication channel model with low path loss based on evanescent wave", *Radioengineering*, Vol. 27 No. 2, pp. 431-439.

Takizawa, K., Suga, R., Matsuda, T. and Kojima, F. (2021), "Underwater MIMO communications by RF signals: capacity analysis, simulations, and experiment", *2021 Joint European Conference on Networks and Communications & 6G Summit (EuCNC/6G Summit), 2021*, pp. 460-465.

Trung, H.D. and Van Duc, N. (2011), "An analysis of MIMO-OFDM for underwater communications", *3rd International Congress on Ultra Modern Telecommunications and Control Systems and Workshops*, ICUMT, 2011, pp. 1-4.

Van Walree, P.A. and Otnes, R. (2013), "Ultrawideband underwater acoustic communication channels", *IEEE Journal of Oceanic Engineering*, Vol. 38 No. 4, pp. 678-688.

Yoshida, H., Iwakiri, N., Fukuda, T., Deguchi, M. and Onogi, S. (2015), "Measurements of underwater electromagnetic

wave propagation", *IEEE Underwater Technology. UT 2015*, No. 2, p. 20215.

Further reading

Sendra, S., Lloret, J., Rodrigues, J.J.P.C. and Aguiar, J.M. (2013), "Underwater wireless communications in freshwater at 2.4 GHz", *IEEE Communications Letters*, Vol. 17 No. 9, pp. 1794-1797.

Hattab, G., El-Tarhuni, M., Al-Ali, M., Joudeh, T. and Qaddoumi, N. (2013), "An underwater wireless sensor network with realistic radio frequency path loss smodel", *International Journal Distrib. Sensor Networks*, Vol. 2013.

Appendix 1. Electromagnetic wave velocity in buffer and water

The electromagnetic wave velocity in dielectric medium c' is:

$$c' = f \cdot \lambda' \tag{12}$$

where λ' is the wavelength in the dielectric. Here, λ' is determined by:

$$\lambda' = \frac{\lambda_0}{\left(\varepsilon_r^2 + \left(\frac{\sigma}{(\omega\varepsilon_0)^2}\right)\right)^{1/4}} \tag{13}$$

where λ_0 is the wavelength in the atmosphere, ε_r is the relative permittivity of the medium, σ is the conductivity of medium and is ω is the radial frequency. The wave velocity in the proposed buffer-layer and water is summarized in Table A1.

Table A1 Comparison of wave velocity in buffer and water at several frequencies

Frequency	Wave velocity (ms^{-1}) In buffer	In water
400 MHz	9.52×10^7	3.33×10^7
500 MHz	9.71×10^7	3.33×10^7
600 MHz	9.81×10^7	3.33×10^7

About the authors

Hanisah Mohd Zali was born in Johor, Malaysia. She received her B.Eng in Electronics (Communication) from Universiti Teknologi Mara (UiTM) Penang in 2012 and M.Sc in Electrical Engineering from Universiti Teknologi Mara Shah Alam, Malaysia in 2018. She has experience working as an assistant lecturer. She is currently pursuing her PhD degree in UiTM. Her research interest includes underwater antenna, plasma antenna and electromagnetic waves applications.

Idnin Pasya is a member of Microwave Research Institute, and the Faculty of Electrical Engineering, Universiti Teknologi MARA. He received the B. E. and M. E. degrees in Information and Communication Engineering from Tokyo Denki University in 2004 and 2006, respectively, and his Ph.D. in Communication Engineering from the same university in 2015. Previously, he worked as an Engineer in Toshiba PC & Network, Tokyo, Japan, from 2006 to 2009, and Pradonet Technology Sdn. Bhd. as Senior Product Engineer in 2009, before joining UiTM in the same year. Dr. Idnin received the IEEE MTT Best Paper Award in 2014 IEEE Radio and Wireless Symposium, held in California, USA. He contributed to IEEE as an executive committee for IEEE AP/MTT/EMC Joint Chapter for the year 2017-2020. Dr. Idnin is also an active member of SIRIM Technical Committee on "Electromagnetic Field" (TC/E/6) for the year 2016-2020. His current research areas are wideband antennas and communication systems, underwater EMW propagation and communication, and MIMO radar and its applications. Idnin Pasya is the corresponding author and can be contacted at: idnin@salam.uitm.edu.my

Miyuki Hirose received here Msc and PhD degree in Information and Communication Engineering from Tokyo Denki University in 2014, and 2017, respectively. She is currently working as Assistant Professor at the School of Science and Technology for Future Life, Tokyo Denki University. Dr. Hirose's current research interests are propagation channel modelling of various wideband communication systems, radar remote sensing, as well as physical layer and hardware security in information systems.

Nurulazlina Ramli She received the B.Eng. degree in electrical engineering (telecommunication) from the 8 Universiti Teknologi Malaysia (UTM), Malaysia in 2008, the M. Sc. degree in telecommunication and information engineering, and the Ph.D. degree in electrical engineering from the Universiti Teknologi Mara (UiTM), Shah Alam, Malaysia, in 2011 and 2015 respectively. Currently, she is a lecturer with the Faculty of Engineering, Built Environment, and Information Technology (FoEBEIT), SEGi University, Malaysia since Sept. 2015. Her research interests include the areas of communication antenna design, reconfigurable/wearable antenna, electromagnetic radiation analysis, indoor/outdoor propagation modeling, dielectric resonator antenna and wireless power transfer.

For instructions on how to order reprints of this article, please visit our website:
www.emeraldgrouppublishing.com/licensing/reprints.htm
Or contact us for further details: **permissions@emeraldinsight.com**